12th Brazilian Congress of Manufacturing Engineering
May 10th-12th, 2023, Brasilia, DF, Brazil

DEVELOPMENT OF A WORKPIECE TEMPERATURE MEASURING DEVICE FOR RADIAL TURNING

Theodor Rucker van Caspel
Matheus Macedo de Roma
Michel Reis Pedreira Muniz Tavares
Claudio Abilio da Silveira
Rolf Bertrand Schroeter
Universidade Federal de Santa Catarina (UFSC), Laboratório Mecânica de Precisão (LMP), Departamento de Engenharia Mecânica. Rua Eng. Agronômico Andrei Cristian Ferreira, Trindade, CEP: 88040-900, Florianópolis - SC, Brasil.
theodorcaspel@gmail.com
matheus.roma99@outlook.com
michel.tavares@posgrad.ufsc.br
claudio.silveira@posgrad.ufsc.br
rolf.schroeter@ufsc.br

Abstract. *During the machining with a defined tool geometry, the machining force can decrease when the temperature in the cutting zone increases. This mostly occurs due to a material softening that happens if the heat conduction allows it. In recent studies, the passive and cutting force components decreased at constant cutting speeds during the hard radial turning of the AISI 52100 HC 60. To confirm if there is still a temperature variation even at constant cutting speed, there was a need to measure the temperature along the process. Hence the objective of this work was to develop and test a temperature measuring device capable of measuring the temperature at different points of the workpiece during the radial turning. The developed device uses a prototyping platform as a basis and thermocouples embedded in the workpiece to measure temperature. The device was divided into three systems, acquisition, amplification, and fastening. The acquisition system was responsible for the control interface and data storage and was composed of the prototyping platform a microSD module, buttons, and LEDs. The amplification system was responsible for amplifying the thermocouples signal and was composed of instrumentation amplifiers, thermocouples, and a thermistor. The fastening system was responsible for holding the other systems inside the lathe chuck so the device would rotate with the workpiece and was composed of an aluminum alloy case, and PVC tube section covered by rubber. Each system was projected and tested before a prototype was assembled. The prototype was capable of sample rates of 1 kHz in four channels, three thermocouples channels, and a thermistor channel for compensation. During the validation, it was determined that the total errors are between 15 to 50 ºC. The temperature measuring device prototype was used to measure temperature during the radial turning of SAE 1040 steel. Though the prototype was able to measure the temperature, it presented failure modes. The most significant ones were the failure in the connection between the thermocouple and the amplification system, and wear in the fastening system. The former caused by incompatibility between the solder and thermocouple wires was solved by adding an intermediary wire. The latter was caused by wear on the fastening system and can be solved by redesigning the fastening system or by making the worn part replaceable.*

Keywords: *machining; radial turning; temperature measurement.*

1. INTRODUCTION

Many high performance parts as well as injection and conformation molds are fabricated of material with elevated hardness (Mohruni *et al*., 2018). Many of those parts are subjected to grinding processes to attain their required dimensional precision and surface quality, but since the 1980s this process started to be replaced by hard turning for many parts. This is happening because hard turning usually has a lower cost, lower preparation time, more flexibility to part geometry, greater removal rate, and can be done without fluid (Mohruni *et al*., 2018). Although hard turning has many advantages it still has drawbacks, such as process reliability, surface quality, and the generation of residual tensile stress (Klocke *et al.*, 2005).

Recent works in radial turning of AISI 52100 HC60 using PCBN tools has been conducted. In the research of Camargo (2019), it was revealed that there was a decrease in machining forces during a single pass. This was exacerbated by tool wear and happened with constant cutting parameters. In the research of Bortoli (2019), it was found that there was an increase in the formation of white layer in regions closer to the workpiece center. Both results indicated that there was an increase in process temperature (Griffiths, 2001; Klocke, 2011). This generated a demand to measure the temperature during this process.

Due to the supposed temperature increase occurring with constant cutting parameters, it was suspected that the increase could have a relation with the increase of spindle rotation required to maintain constant cutting speed in radial turning and the increase could be a result of the shortening of the interval between tool passage in a region, reducing the cooling time of that region. Because of this, measuring the temperature in fixed regions of the workpiece could reveal details of the involved phenomena.

As this research would be exploratory and because of a limitation in resources, it was decided that a temperature measuring device would be developed. The objective of this research was to develop a device capable of measuring temperature in the workpiece during the process of radial turning.

2. METHODOLOGY

The developed device was done as part of the work of van Caspel (2022) and was composed of three systems: Acquisition, Amplification, and Fastening. Each system was simulated and tested independently before a prototype was assembled.

2.1 Requirements

The first step in the development of the device was to determine the requirements. As the main objective of the device was to determine if there was a temperature variation during radial turning and with the intention of measuring the temperature in the workpiece, the temperature should be measured at more than one point.

Due to limited resources and the exploratory character of the research, there would need to be a compromise between precision and cost. Davies *et al.* (2007) reported that the best precision obtained at the time was an error above 10 ºC, for the first prototype of the device an error below 50 ºC was considered acceptable.

During previous works, the highest lathe spindle rotation achieved during cut was close to 3000 rpm (50 Hz), as the expected signal would be generated due to the rotation the system must be capable of acquiring signals with at least the rotation frequency. It is recommended that a signal be acquired with a frequency four times greater than the low pass filter cutoff frequency (Shin and Hammond, 2008). Although no filter was used in the first tests so that no unpredicted signal is removed, a filter should be added in the future and the cutoff frequency of the low pass filter should be at least above 50 Hz, so the acquisition should be done with at least 200 Hz of sample rate.

During the machining of AISI 52100, the temperature can reach close to 900 ºC (Chen *et al*., 2017) so the device should be capable of measuring temperatures up to 1000 ºC to prevent saturation. As temperature radiation emission methods require that the measured body be stationary to the measuring device, their use was not considered.

Due to the cost limitations and requirements, it was decided that the measurement would be made by using type K thermocouples embedded in the workpiece and that the device would be rotated with the workpiece during acquisition. The device would be fastened to the lathe chuck, in the central hole, and would store data internally during the process, because of that the device would need to be compact. The device would be designed around an Arduino® Nano board because it is a compact prototyping platform.

2.2 Acquisition system

The acquisition system is responsible for data acquisition, data storage, interface, and control. The device programming was done using the Arduino Integrated Development Environment (IDE) available on the Arduino official website (Arduino, 2022) and used the standard libraries and the SdFat library (Greiman, 2022). The two main components of the acquisition system are the Arduino Nano® Board and the microSD card module. The algorithm used was composed of an interrupt function responsible for the data acquisition and the main function responsible for the data storage.

Many configurations of this system were tested to define the best number of input channels for acquisition and the higher sample rate possible without buffer overflow. The more stable configurations were assembled in protoboards and tested with a function generator to check if the frequency used for the interrupt function translated to the correct sample rate.

The configuration chosen used four analog input channels with a sample rate of 1 kHz. The main limiter to sample rate and the number of channels was identified as being the speed of data transfer between the Arduino and the MicroSD module using a Serial Peripheral Interface (SPI) connection. There were fluctuations in the data transfer speed that caused frequent buffer overload at higher sample rate.

As the prototyping board uses 10 bits Analog Digital Converters (ADC) and a variable cannot be stored in fractions of bytes, there would be a waste of 6 bits in each sample for each channel. To reduce this waste, three of the signals were concatenated in a single 32 bits variable (instead of using three 16 bits variables). As the time functions did not work with the interrupt function used, the last variable was concatenated with a 6 bits counter. These concatenations reduced the size of the data for each sample from 8 to 6 Bytes. Figure 1 shows the electrical schematic of the acquisition system.

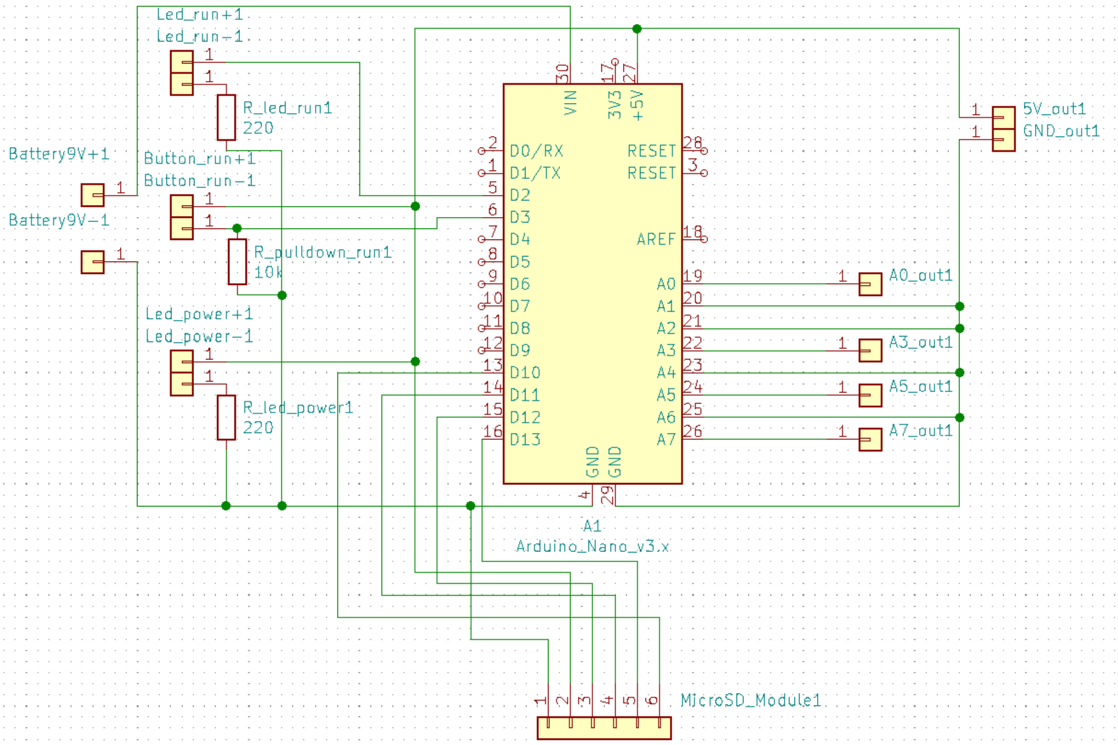

Figure 1. Electrical schematic of the acquisition system

In the center is the Arduino Nano® responsible for the control of the Device. On the left are the connections for the components responsible for the interface, including buttons, LEDs, and the battery. On the bottom is the MicroSD module responsible for data storage. On the right is the connection to the amplification system, to share GND and 5 V signals and to receive the inputs for acquisition. After all the tests. A Printed Circuit Board (PCB) board for the acquisition system was designed and manufactured.

2.3 Amplification system

The amplification system is responsible for the conditioning of the signal in a way that is appropriate so that it can be acquired by the acquisition system. In the first prototype, no filters will be added decreasing the chance of any unpredicted signal being masked. The voltage range generated by the type K thermocouple between zero and 1200 ºC is approximately from zero to 50 mV (Garrity, 2000) while the input ranges from the Arduino Nano® ADCs is from zero to 5 V. With these values, a gain of 100 would maximize the measurement sensibility without sacrificing the measuring range.

The instrumentation amplifier INA333 from Texas Instruments was chosen to amplify the thermocouple signals. One motive for this choice was that it could work in a single supply mode, which eliminated the risk of generating a negative output voltage, that could damage the ADCs. It is also a low-power amplifier, allowing it to be powered by the Arduino. It also is a rail-to-rail amplifier, meaning that the signal saturation is very close to the supply.

An amplification circuit was designed and tested using simulation software provided by Texas Instruments called Tina-TI. After this, one amplifier was mounted in an adaptor so it could be tested using a protoboard. An uncontrolled heat source was used to heat a thermocouple to generate a small enough signal to test the amplification.

The amplification circuit was repeated for three of the four channels. The last channel was used for the compensation for the cold junctions of the thermocouples. For this, a voltage divisor with a thermistor and a resistor was used. Figure 2 shows the electric schematic of the amplification system.

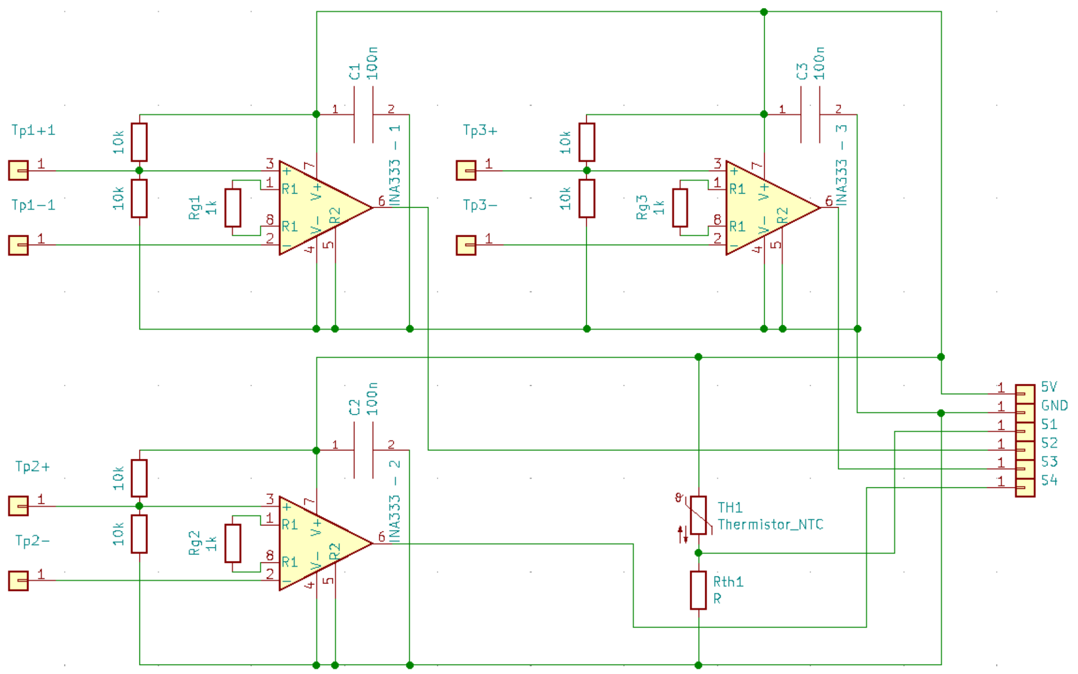

Figure 2. Electrical schematic of the amplification system

The amplification circuit for the thermocouples can be seen in the upper left, upper right, and lower left. The thermistor voltage divider can be seen in the lower right. On the extreme right, the connections to the acquisition system can be seen.

2.4 Fastening system

The fastening system is responsible for maintaining the device stationary in relation to the lathe chuck. The fastening system also acts as a case for the device. As the device would be used in the central hole of the lathe chuck, the fastening system needs to guarantee that the device would rotate at the same frequency as the chuck and that it would not leave the hole and neither go deeper. To minimize centrifugal effects that could damage the electronic systems the fastening system should hold the other two systems as close to the chuck rotation axis as possible. Figure 3 shows the acquisition and amplifications systems inside the case.

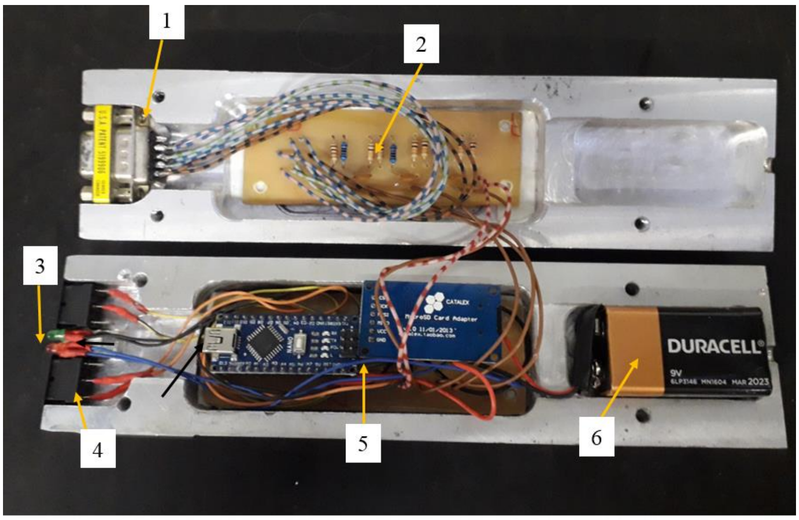

1-DB9 Connector
2-Amplification system
3-LEDs
4-Buttons
5-Acquisition system
6-Battery

Figure 3. Acquisition and amplification system inside the case.

The chosen solution was for the fastening system to be composed of a cylinder with internal slots to support all the systems and components with a pressure clamp on its extremity to hold it inside the chuck hole. The cylinder was fabricated using Aluminum alloy 6061 and was longitudinally sectioned, during use it would be held closed by four M4 screws. Figure 4 shows the cylinder and pressure clamp.

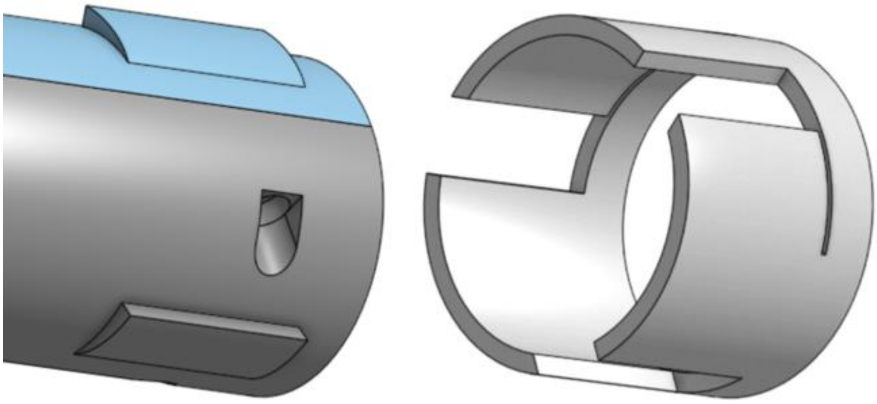

Figure 4. View of the cylinder and pressure clamp

The pressure clamp was composed of a PVC ring over a section of the cylinder, this section of the cylinder has ramping protrusions that would fit in indentations on the rig. When the cylinder is rotated while maintaining the ring stationary, the protrusions would be pushed below the PVC causing it to expand. The direction of the ramping protrusions was chosen so that with the rotation of the lathe the clamp would tend to fasten, to reduce the risk of the device coming loose during an experiment. The fastening system was tested with rotations up to 4500 rpm in the intended direction and in reverse before the slots for the other components were machined. Figure 5 shows the device fastened to the lathe's chuck.

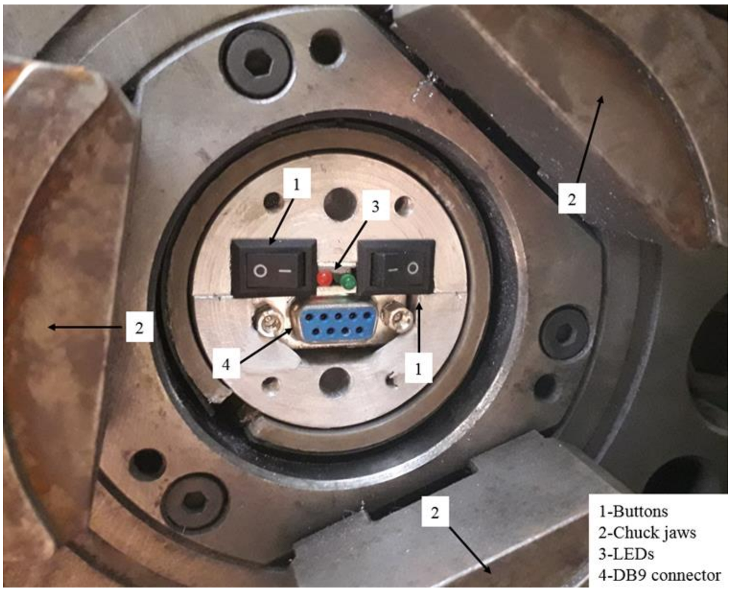

Figure 5. Device fastened to the lathe's chuck.

2.5 Workpiece preparation

The workpieces used were 100 mm diameter discs with a 24 mm diameter hole in their center and 15 mm thick. They were made of AISI 1040 steel. Three holes were made using Electrical Discharge Machining (EDM) with a 1.6 mm electrode and approximately 12.7 mm deep and positioned in a line at 15, 30, and 45 mm from the center of the disc.

In each hole, a thermocouple was embedded and fixed with cyanoacrylate glue. Each thermocouple was a type K thermocouple made with 0.51 mm wires with their points welded with capacitor discharge welding, using equipment developed by Silveira (2020). The length of the wires was covered with temperature resistant polyimide tape to prevent the formation of false joints. Figure 6 shows the assembled workpiece.

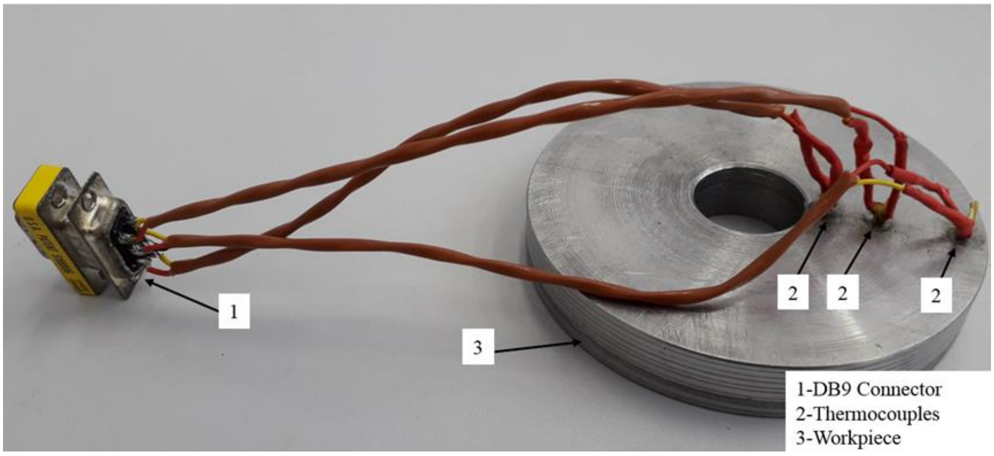

Figure 6. Assembled workpiece.

After the thermocouples were embedded, thermocouple wires were used to connect the thermocouples to a DB9 connector. A thermistor was mounted in the DB9 connector to measure the temperature of the cold junctions for compensation.

2.6 Data translation

The raw data obtained by the device is in the form of two columns of data, one column with 16 bits variables and another with 32 bits variables. To translate this raw data to the temperature signal of the three thermocouples an algorithm was made using the software Matlab®. Figure 7 shows a simplified schematic representation of the algorithm.

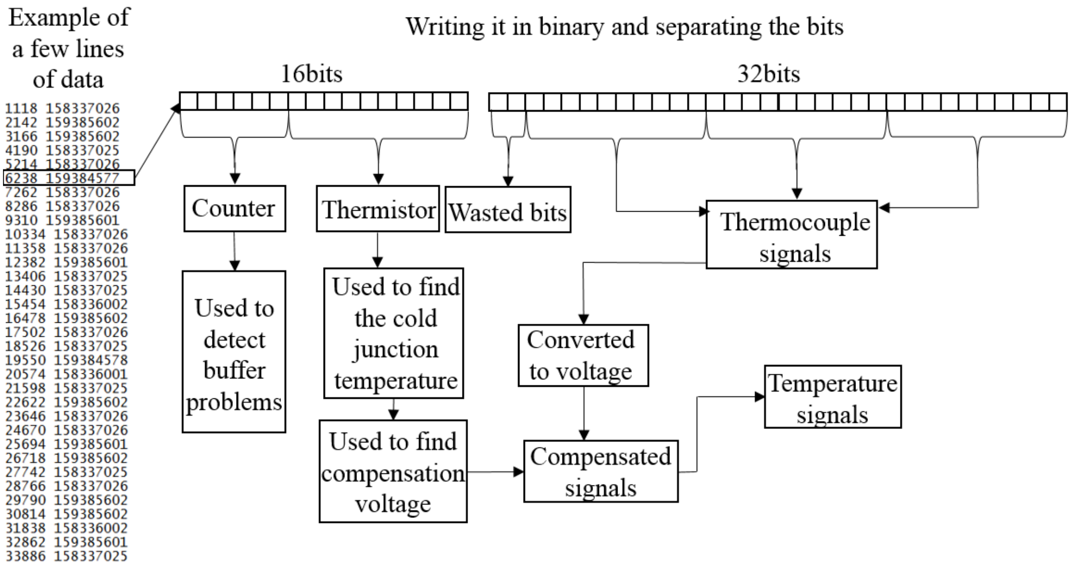

Figure 7. Schematic representation of the data translation algorithm.

The algorithm separates the concatenated variables in each line generation into a total of five signals: Counter, thermistor signal, and three thermocouple signals. The Counter is analyzed to check if there was any buffer overload. The thermistor signal is converted to a temperature signal and used to determine the compensation for each data point. The thermocouple signals are converted to voltage signals, compensated, and then converted to temperature signals using a voltage temperature conversion table (Garrity, 2000).

2.7 Validation

Due to the limited resources and lack of access to calibration equipment with recent calibration, it was decided that a full calibration would not be done for the first prototype and a simpler validation would be done with accessible equipment. The validation was based on the GUM method (JCGM, 2008) and was done in two steps.

For the first step, a Multicalibrator Omega CLD-II was used as a voltage source. Voltage from 0 to 50 mV with 5 mV steps was measured using each thermocouple channel of the device acquiring 5000 data points per step. With this, it was possible to determine each amplifier's saturation voltage and exact gain. With the gain, it was possible to calculate systematic and random errors for each step on non-saturated signals.

The second step consisted in using an oven Omega CL552 as a heat source to test the device using thermocouples in temperatures up to 1100 ºC. The systematic errors remained below 20 ºC for all channels for temperatures up to 300 ºC and below 50 ºC up to 1100 ºC, this systematic errors may have been exacerbated due to improper positioning between the oven's internal thermocouple and the device’s thermocouples due to the oven being designed to be used with probes instead of bare wire thermocouples. The random errors remained beneath 3.0 ºC.

One channel presented a limited measuring range (200 to 800 ºC) due to amplifier saturation. Another channel presented a measuring range between 10 and 900 ºC and the last one presented a range between 5 and 1050 ºC. The measuring ranges consider a cold joint at 0 ºC. These limited measuring ranges may be caused by failures during the assembly of the PCBs.

3. RESULTS

The device’s prototype was capable of measuring temperature during experiments involving the radial turning of AISI 1040 with carbide uncoated tools. It was identified that the distance between the thermocouples and the machined surface and the heat generated during the process had a great impact on the intensity and type of signals acquired.

When there was low process heat and with a greater distance between the thermocouple and the machined surface no signal above saturation was detected. When there was more process heat or the thermocouple became closer to the machined surface, a clear increase in temperature over time, measured in seconds, was detected. When the heat generated was greater and the thermocouple was closer to the machined surface, pulsed signals with the same frequency as the spindle rotation superimposed with the previous signal were detected. The temperature variation in the pulsed signal was much greater than in the previous signal. This means that the thermocouple should be inserted as close as possible to the machined surface.

Although the sample rate was enough to capture the pulsed signal frequency, due to the temperature increase being so sudden and followed by a sharp temperature drop, a higher sample rate would be necessary to capture to guarantee that enough of the curve was captured to determine the peak temperature.

3.1 Failure Analisys

Although the device prototype was able to measure the temperature on the workpiece during radial turning, this did not occur without failures. Some of these failures were already solved, but some were not solved until the publication of this research due to limitations of resources or time. There were four main failures identified in the prototype that should be eliminated or at least mitigated.

The first failure that will be discussed is related to the assembly of the workpiece, more specifically the connector. In the first tests, the thermocouple wire was directly connected to the connector using tin solder and no case for the connector was used due to a lack of space between the device and the workpiece when mounted in the lathe. Due to chemical incompatibility between tin and the thermocouple materials the solder failed during some of the experiments. Although there was no force pulling the connector and having a tight fit, in one experiment the connector came loose.

To solve this failure with the connector, an intermediate copper wire was used between the thermocouple wire and the connector and a case that could be cut to fit between the workpiece and the device was acquired. The intermediate wire was soldered with tin to the connector and welded to the thermocouple wire with capacitor discharge welding. The new case was cut, and the screws present in the case allowed for a more secure connection.

The second failure is related to signal saturation and compensation. At the start of each experiment, both joints of the thermocouples were at the same temperature, theoretically generating a zero volts signal. Due to amplification saturation, the real signal was always above zero volts and after compensation, the measured temperature appeared as being a few degrees above ambient temperature.

During the experiment, the measuring joint of the thermocouple would be heated as the heat generated by the process reached the specific thermocouple. The cold joints and the thermistor would be heated by conduction by the thermocouple wire. As not all thermocouples were heated at the same time, the thermistor could be heated and the compensation changed without the thermocouples presenting a signal above saturation, and this causes the appearance of a signal due to the variation of compensation while the thermocouple signals were still saturated.

To correct this failure, it is necessary to alter both the amplification and acquisition systems. One solution would be to use a dual supply amplifier and guarantee that it would never be saturated in the measuring range. This solution would require changes in the acquisition system because the ADCs of the Arduino Nano® cannot acquire negative voltages and could be damaged by them. Another solution would be to somehow cool the cold junction so that the thermocouple signal is always above the current saturation. Neither solution was yet implemented due to limitations of time.

The third failure is related to wear in the fastening system. To be able to collect the data from the experiments the device prototype needs to be removed from the lathe and opened to access the Arduino Nano®. After several experiments, the fastening system started to show wear. This wear caused a vibration that prejudiced the acquisition and presented a risk.

Resolving this failure would require a redesign of the fastening system. There are two routes considered for the redesign. The first is to change the fastening system concept and make it more durable. The second is to determine components that would become worn to be substituted.

The fourth failure is related to the buffer and the acquisition. During the initial tests in a protoboard, the acquisition system could maintain a 1 kHz sample rate in four channels without overflow. During the experiments using the same rate and the same number of channels, the system started presenting buffer overflow at a few points. Due to a lack of resources and time, it was not possible to assemble another prototype to test if the failure was due to the assembly. The failure could also be due to the rotation of the device.

The simplest way to resolve this failure is to reduce the sample rate or reduce the number of channels. This would require adjustments to the algorithms and redoing the tests to guarantee that the changes did not cause further failures. This would also be detrimental to the acquisition of the pulsed signals. Another solution would be to work on what is limiting the sample rate, and the fluctuation of that transference rate between the Arduino Nano® and the MicroSD module. To do that two solutions have been proposed. The first is to use a prototyping platform with more Random Access Memory (RAM) to work with a greater number of buffers. The second solution would be to use a prototyping platform with native MicroSD, as these can transfer data much faster than through the SPI connection.

4. CONCLUSION

The developed device prototype was capable of measuring temperature in the workpiece during radial turning. It was better able to acquire the signals with the thermocouples placed as close to the surface as possible. Despite this, the prototype presented a few failures that must be corrected. Solutions for the failures were proposed and applied when possible.

5. REFERENCES

Arduino, 2022. Arduino Website. 1 fev. 2022. < https://www.arduino.cc/>.

Bortoli, G. A. de, 2019. Avaliação da integridade da superfície usinada em função do desgaste da ferramenta de PCBN no torneamento radial do aço AISI 52100. Trabalho de conlusão de curso, Universidade Federal de Santa Catarina, Florianópolis.

Camargo, F. J. de, 2019. Influência da direção de corte na progressão do desgaste de ferramentas de PCBN aplicadas no torneamento do aço AISI 52100 temperado e revenido. Dissertação de mestrado, Universidade Federal de Santa Catarina, Florianópolis.

Chen, L., Tai, B. L., Chaudhari, R. G.; Song, X.; Shih, A. J., 2017 Machined surface temperature in hard turning. *International Journal of Machine Tools and Manufacture*, v. 121, november 2016, p. 10–21.

Davies, M. A., Ueda, T., M'saoubi, R.; Mullany, B., Cooke, A. L., 2007. On The Measurement of Temperature in Material Removal Processes. *CIRP Annals - Manufacturing Technology*, v. 56, n. 2, p. 581–604.

Garrity, K., 2022. *NIST ITS-90 Thermocouple Database - SRD 60.* 11 may. <https://doi.org/10.18434/T4S888>.

Greiman, B., 2022 SdFat library. 11 may. <https://github.com/greiman/SdFat>.

Griffiths, B. J., 2001. Manufacturing surface technology. Penton Press, London, 1th edition.

Joint Committee for Guides in Metrology ISBN, 2008. Evaluation of measurement data — Guide to the expression of uncertainty in measurement. *International Organization for Standardization Geneva ISB*.

Garrity, K., (2000), NIST ITS-90 Thermocouple Database - SRD 60, National Institute of Standards and Technology, https://doi.org/10.18434/T4S888 (Accessed 2022-10-19)

Klocke, F., Brinkmeier, E., Weinert, K., 2005. Capability Profile of Hard Cutting and Grinding Processes. *CIRP Annals - Manufacturing Technology*, v. 54, n. 2, p. 22–45.

Klocke, F., 2011 Manufacturing Processes 1. Springer, Berlin, 1th edition.

Mohruni, A. S., Yanis, M., Kurniawan, E., 2018. Development of surface roughness prediction model for hard turning on AISI D2 steel using cubic boron nitride insert. *Jurnal Teknologi*, v. 80, n. 1, p. 173–178.

Shin, K., Hammond, J., 2008. Fundamentals of signal processing for sound and vibration engineers. John Wiley & Sons, Ltd.

Silveira, C. A. da, 2020. Análise da movimentação síncrona e simultânea entre scanner galvanométrico e eixos lineares em aplicações laser. Tese de Doutorado, Universidade Federal de Santa Catarina, Florianópolis.

van Caspel, T. R., 2022. Workpiece temperature measurement in radial turning. Dissertação de mestrado, Universidade Federal de Santa Catarina, Florianópolis.

6. RESPONSIBILITY NOTICE